Chemical Engineering Journal 470 (2023) 143905

Contents lists available at ScienceDirect

Chemical Engineering Journal

journal homepage: www.elsevier.com/locate/cej

Competitive and synergistic effects of metal adsorption in water remediation processes mediated by hybrid copolymers

Amanda Haro-Martínez [a,1], Rocío Arroyo-Carrasco [a,1], Laura Galván [b], Ana Sayago [c], Antonio A. Cuadri [d], José Enrique Martín-Alfonso [d], Ángeles Trujillo-Reyes [e], Fernando G. Fermoso [e], Juan Cubero-Cardoso [a,e,*], Juan Urbano [a,*]

[a] Laboratory of Sustainable and Circular Technology. CIDERTA and Chemistry department, Faculty of Experimental Sciences. Campus de "El Carmen", University of Huelva, 21071 Huelva, Spain
[b] Department of Agroforestry Sciences, University of Huelva, Avda. Fuerzas Armadas s/n, Huelva 21071, Spain
[c] AgriFood Laboratory, Faculty of Experimental Sciences, University of Huelva, 21007 Huelva, Spain
[d] Department of Chemical Engineering and Materials Science, Campus de "El Carmen", University of Huelva, Chemical Product and Process Technology Research Center, (Pro2TecS) 21071 Huelva, Spain
[e] Instituto de Grasa, Spanish National Research Council (CSIC), Ctra. de Utrera, km. 1, 41013 Seville, Spain

ARTICLE INFO

Keywords:
Adsorption
Green chemistry
Inverse Vulcanization
Kinetic study
Water remediation

ABSTRACT

Copolymers based on vegetable oils and sulfur have recently been developed using the inverse vulcanization technique for water remediation. This study aimed to create a copolymer with heteroatoms, such as nitrogen, to improve adsorption efficiency and examine the competition and synergy between heavy metals in the adsorption process. FTIR, ^{1}H NMR, solid ^{13}C NMR, zeta potential, nitrogen adsorption, Elemental analysis, TEM, and SEM were used to characterize the copolymers synthesized. Once metal adsorption was optimized using the synthesized copolymers, a comparative adsorption study was conducted for the removal of individual heavy metals, Cd^{2+}, Pb^{2+}, Zn^{2+}, Mn^{2+}, and Cu^{2+} (100 mg/L), using two copolymers, S/CO:80/20 and S/CO/TAA:80/14/6. The copolymers exhibited a higher affinity for soft metals, such as Cd^{2+}, Pb^{2+}, and Cu^{2+}, when they are individually and in a mixture. After 1 h, the S/CO:80/20 copolymer removed 47%, 40%, and 13% of these metals. While with the S/CO/TAA:80/14/6 copolymer removal increased to 10%, 24%, and 53%, respectively respect to S/CO:80/20 copolymer. The introduction of heteroatoms in the copolymers improved their removal efficiency, particularly for heavy metals like Pb^{2+}. Overall, this study demonstrates a promising approach for sustainable water remediation using copolymers.

1. Introduction

Water quality has always been crucial for human health, but uncontrolled pollution discharges to water and soil have been a severe environmental problem due to industrial development and general human ignorance [1,2]. Recently, concern for the environment has led to the adoption of legislative measures and pollutant elimination techniques, including the establishment of a community framework for action in the field of water policy through Directive 2000/60/CE. The directive aims to protect inland surface, transitional and coastal waters, as well as groundwater [3]. Pollutants in water can be classified as organic, inorganic, and biological, with heavy metals being the most common inorganics [4–6], and pesticides, herbicides, fats, oils, detergents, lignin, and drugs being the organic compounds. Biological pollutants refer to microorganisms capable of causing damage to health [7].

Currently, there are different traditional and novel techniques for water purification, such as chemical precipitation, sedimentation, flotation, filtration, and reverse osmosis. However, the study of new techniques and the use of new, more sustainable materials are required because, in many cases, these techniques are quite expensive at an economic and operational level [1,8]. The use of adsorbents to eliminate

* Corresponding authors at: Laboratory of Sustainable and Circular Technology. CIDERTA and Chemistry department, Faculty of Experimental Sciences. Campus de "El Carmen", University of Huelva, 21071 Huelva, Spain.
E-mail addresses: j.cubero@dqcm.uhu.es (J. Cubero-Cardoso), juan.urbano@dqcm.uhu.es (J. Urbano).
[1] First author: both authors contributed equally.

https://doi.org/10.1016/j.cej.2023.143905
Received 14 March 2023; Received in revised form 29 May 2023; Accepted 31 May 2023
Available online 15 June 2023

pollutants in water has recently increased due to the biocompatibility and biodegradability of adsorbents [9]. There are several studies showing the ability of different adsorbent materials to separate, concentrate and purify of various compounds [10,11]. In the same way, external characteristics such as porosity, particle size, irregularities on the surface, impurities, surface area or pH, and temperature can affect the physical adsorption process [10]. A desirable adsorbent material is characterized by being economical, non-toxic, and sustainable with the environment [9] because reducing pollution is essential for conserving the environment [12]. A few years ago, the more commonly used adsorbents were of very different origins, ranging from biomass to minerals such as clays and zeolites, some metal oxides and even fly ash [9,13]. However, the adsorbent materials used for the extraction of organic pollutants and heavy metals most frequently have been activated carbon and copolymeric resins [9].

Recently, absorbent resins derived from sulfur obtained from the process called inverse vulcanization have been revealed. Chung et al. [14] found an elegant method of taking advantage of the reactivity of sulfur with different olefins at temperatures above 159 °C, where radicals are generated by the opening of ring S_8 [15]. In so-called classical vulcanization, elemental sulfur is used in relatively small amounts, and is usually used to cross-link and harden rubbers or other polymers in a high-temperature process. Meanwhile, in the so-called inverse vulcanization, a small amount of unsaturated comonomer joins with sulfur and branches the polysulfide copolymers at high temperatures, forming a copolymer stable to depolymerization. In this way, through inverse vulcanization, stable copolymers with a very high sulfur content (typically 50–90% sulfur by mass) can be obtained. This methodology can be considered of great relevance for Green Chemistry since inverse vulcanization does not require solvents or exogenous reagents in the synthesis of copolymers [16]. Both sulfur and the corresponding olefin are used as comonomers and as a reaction medium, presenting great atomic economy, as previously mentioned, since all the starting material is incorporated into the final product.

These types of copolymers are currently being studied due to their versatility in modifications for different applications, depending mainly on the unsaturated compound used, which would make it possible to obtain adsorbent copolymers to adsorb a wide range of pollutants in water. Unlike elemental sulfur, polysulfide copolymers produced by inverse vulcanization can be processed to have mechanical, chemical, and thermal properties that are complementary to or better than those of elemental sulfur [17]. As previously mentioned, it is necessary to develop sustainable methodologies based on systems that use renewable raw materials. Thus, in recent years, examples of copolymers generated by inverse vulcanization based on vegetable oils or compounds of natural origin have appeared in the literature and have been used successfully in sustainable applications [18]. Cathodes of lithium-sulfur batteries, demonstrating a remarkable specific initial capacity, have been made with a hybrid copolymer based on vegetable oils such as olive, sunflower, and linseed [19]. In addition, these hybrid copolymers have even been used as a controlled source of sulfur for plants and as a fertilizer, with improved oxidation capacity using soybean oil as a comonomer [20]. Similarly, other examples of copolymers generated by inverse vulcanization have been postulated as materials with enhanced antibacterial activity [21–24].

Finally, in addition to these interesting applications, it has been observed that these copolymers formed by inverse vulcanization have an affinity for some metallic cations in solution. Taking into account the HSAB (Hard–Soft–Acid–Base) theory, this behavior occurs because sulfur atoms in the skeleton of the polymer can form covalent bonds with soft Lewis acids in solution; therefore, these copolymers could be used as a promising adsorbent material for subsequent water treatment [25,26]. In general, most examples of hybrid copolymers found in the literature have focused on their great interaction with soft metals such as mercury, either in its liquid or gaseous state, or in other mercurial derivatives [17,25,27–31]. However, the number of examples realizing the adsorption of heavy metals other than mercury is quite low [25,30,32]. In the search for more versatile systems with a greater affinity toward a wider range of metals in solution, it is necessary to adequately design the architecture of the polymer by introducing heteroatoms other than sulfur, which allow anchoring points toward other harder metals.

This work aims to obtain novel copolymeric materials by inverse vulcanization, reusing industrial by-products, for the controlled adsorption of inorganic pollutants in water. Several synthesized polymers have been tested for the absorption of individual metals. Their performance was studied regarding the interplay between synergy and competition during adsorption in solutions containing mixtures of metals mimicking real samples. Furthermore, the research will explore the adsorption affinity of metals with doped copolymers with heteroatoms, such as nitrogen.

2. Materials and methods

2.1. Synthesis of Polysulfide adsorbent

Polysulfide-Co-Castor oil (S/CO copolymer) was prepared with percentage in w/w % of 30/70, 70/30, and 80/20. The mixtures were placed made into a 50 mL vial with a magnetic stir bar. The mixture was stirred thoroughly at 170 °C for 60 min so that the feedstocks were mixed evenly. Additionally, a Polysulfide-Co-Castor oil- Co-tryallylamine (S/CO/TAA copolymer) was made under the same conditions with a percentage of 80/14/6 in w/w/w %.

2.2. Batch metal adsorption experiments

Batch adsorption experiments were carried out in triplicate to check the removal capacity of the prepared samples for Cu^{2+}, Cd^{2+}, Pb^{2+}, Zn^{2+}, and Mn^{2+} in an aqueous solution of 100 mg/L. Different studies have been conducted on the percentage of sulfur, dosage, and kinetics with S/CO:80/20 and S/CO/TAA:80/14/6 copolymers crushed with a coffee grinder. The removal of individual metals at 1 and 24 h adsorption time from different copolymers with a dosage of 50 g/L was studied. Then, dosage (2, 10, 25, 50, and 100 g/L, 1 g copolymers) studies were performed with S/CO:80/20 and S/CO/TAA:80/14/6. Finally, a kinetic study was performed with sulfur at a 100% cero point for 72 h. The removal and quantity of metal ions adsorbed onto copolymers were calculated as follows:

$$\text{Percentage Removal}: \quad q_r = \frac{(C_0 - C_e)}{C_0} x100 \tag{1}$$

$$\text{Amount Adsorbed}: \quad q_e = \frac{(C_0 - C_e)V}{W} \tag{2}$$

where q_e is the amount of metal ion adsorbed per gram of adsorbent, C_0 (mg/L) is the initial metal ion concentration, C_e (mg/L) is the metal ion concentration at time t, W (g) is the mass of the adsorbent, and V (L) is the volume of the solution.

The influence of a mixed-metals solution on the adsorption of the copolymer is carried out using a solution with a known concentration (**Table S1**). Additionally, the mixed-metals solution was brought to pH values of 1.6, 2.6, 3.34, 4.87, and 6.02 to determine their influence on adsorption. Adsorption studies at each pH level were carried out discontinuously and in triplicate. The adsorbent and the solution were in contact in 30 mL vials (1 g of S/CO:80/20 copolymer and 20 mL of mix-metal solution), applying continuous agitation for 24 h and repeating the procedure for each pH level of the study.

2.3. Kinetic study

The adsorption capacity quantification of an adsorbent was carried out by applying the Langmuir and Freundlich isotherm models. The

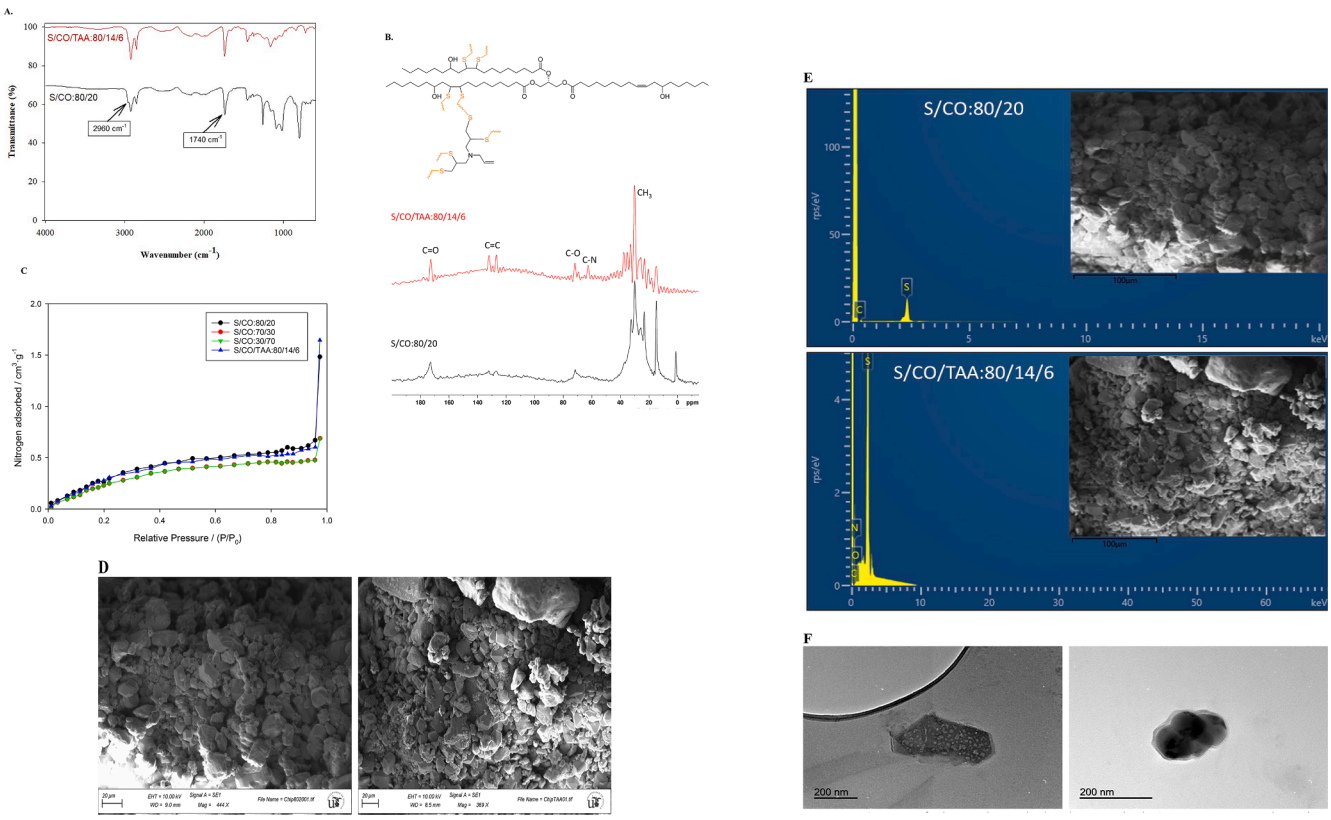

Fig. 1. A) FTIR of S/CO:80/20 and S/CO/TAA:80/14/6 (0.06:0.01:0.06 M ratio). B) solid-state ^{13}C NMR copolymers. C) The N_2 adsorption isotherms (at 77.3 k, 1 bar) of different copolymers. D) SEM Images of S/CO:80/20 and S/CO/TAA:80/14/6 copolymers. E) SEM-EDS spectrum of S/CO:80/20 and S/CO/TAA:80/14/6 copolymers. F) TEM images of S/CO:80/20 and S/CO/TAA:80/14/6 copolymers.

concentrations of each metal were 100, 75, 50, 25, 10, 5 and 1 ppm for 24 h. The Langmuir isotherm assumes that the maximum adsorption corresponds to a saturated monolayer of adsorbate molecules on the surface, the adsorption energy is constant, and there is no transmigration of adsorbate in the plane of the surface [33]. The linear form of the Langmuir equation can be expressed as follows:

$$\frac{C_e}{q_e} = \frac{C_e}{q_{max}} + \frac{1}{q_{max}k_L} \tag{3}$$

where C_e is the equilibrium concentration of metal ions (mg/L), qe is the amount of metal ions adsorbed per unit weight of adsorbed at equilibrium (mg/g), k_L is the Langmuir constant (L/mg), and q_{max} is the maximum adsorption at the monolayer (mg/g).

The linear form of the Freundlich equation can be expressed as follows:

$$\log q_e = \log k_F + \frac{1}{n}\log C_e \tag{4}$$

where C_e is the equilibrium concentration of metal ions (mg/L), q_e is the amount of metal ions adsorbed per unit weight adsorbed at equilibrium (mg/g), k_F is the Freundlich constant and n is the adsorption capacity (mg/g).

The rate of metal adsorption is an important factor, as it provides valuable insights into the reaction pathways and the adsorption mechanism [34]. The two most common models used in describing the reaction kinetics include the pseudo-first-order and pseudo-second-order models. The pseudo-first-order kinetic model was proposed by Lagergren [35]. The general form of the model is expressed as follows:

$$\frac{dq_t}{dt} = k_1(q_e - q_t) \tag{5}$$

where k_1 is the rate constant (min $^{-1}$), q_t is the amount of metal ion adsorbed at time t (mg/g) and q_e is the value at equilibrium (mg/g). After definite integration by applying boundary conditions $q_t = 0$ at t = 0 and $q_t = q_t$ at t = t, the integrated form becomes:

$$\ln q_e - \ln q_t = \ln q_e - k_1 t \tag{6}$$

The pseudo-second-order kinetic model proposed by Ho and McKay (Ho and McKay, 1999)[36] assumes that adsorption follows second-order chemisorption. The general form can be written as follows:

$$\frac{dq_t}{dt} = k_2(q_e - q_t)^2 \tag{7}$$

where k_2 is the pseudo-second-order rate constant (g/mg min), q_t is the amount of metal ions adsorbed at time t (mg/g), and q_e is the value at equilibrium (mg/g). The linear form can be expressed as follows:

$$\frac{t}{q_t} = \frac{1}{k_2 q_e{}^2} + \frac{t}{q_e} \tag{8}$$

2.4. Characterization of Polysulfide adsorbent

Nuclear magnetic resonance spectroscopy (^1H NMR) of the S/CO/TAA copolymer sample was captured at 500 MHz using a Varian Mercury 500 spectrometer, and deuterated pyridine (Py-D5) was employed as a solvent. Solid-State ^{13}C Nuclear Magnetic Resonance (NMR) Spectroscopy was acquired with a Bruker Avance III HD 400 MHz (Rheinstetten, Germany) at a frequency of 100.63 MHz using zirconium rotors with a 4 mm outside diameter.

Fourier transform infrared (FTIR) spectra were recorded in absorption mode in the wavenumber range of 400–4000 cm^{-1} with a resolution of 4 cm^{-1} using an FT/IR-4200 instrument (Jasco Analytical Instrument, Japan). A total of 46 scans were performed on each sample in

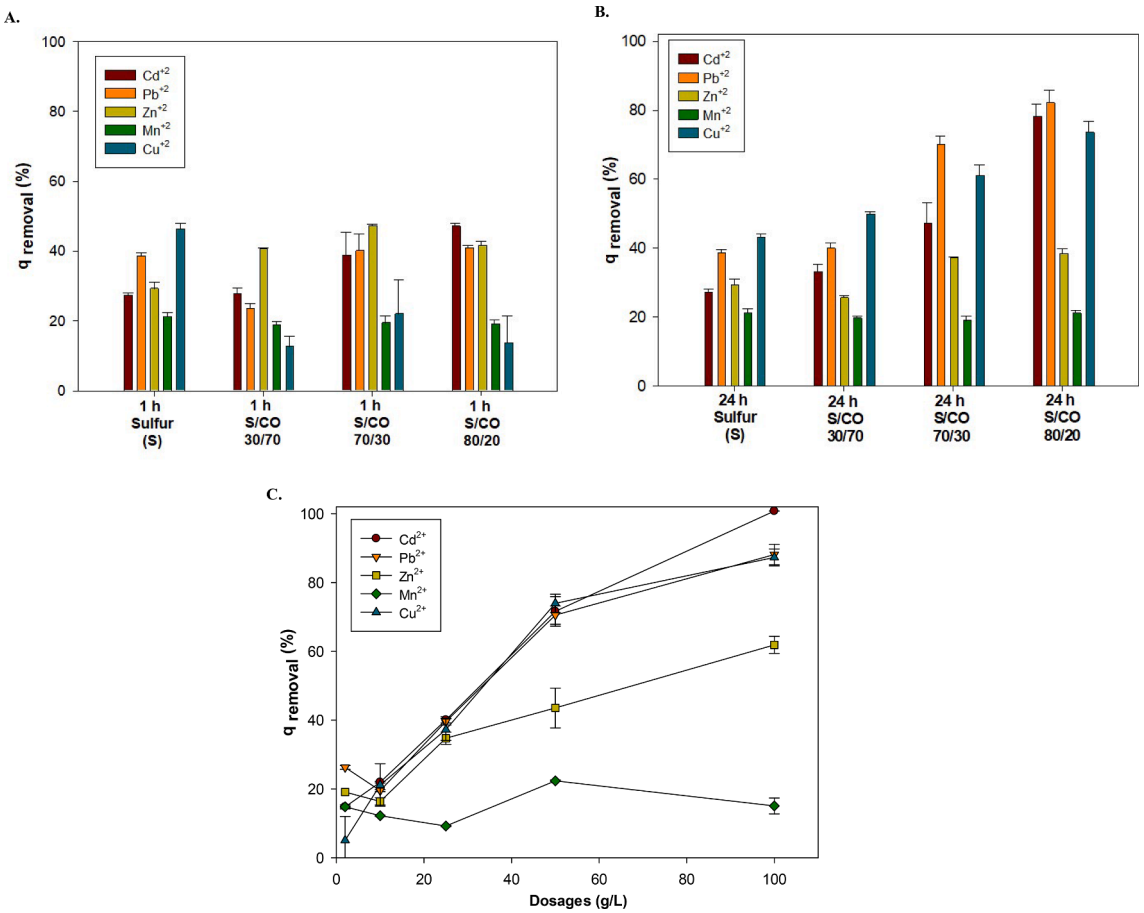

Fig. 2. Percentage of metals removal with different adsorbent from S/CO copolymer and 100 % sulfur during A) 1 h, B) 24 h, and C) Effect of adsorbent dosage by S/CO:80/20 copolymer at 24 h.

transmission mode. Additionally, the attenuated total single reflection accessory with a diamond crystal is used for surface FTIR analysis of thin films.

The Zetasizer Nano ZSP instrument (Malvern Instruments Ltd., UK) was used to analyse the zeta potential of the copolymers. The samples were previously diluted in water and the measurements were recorded in triplicate at 25 °C. Surface areas were measured by nitrogen adsorption at 77.3 K, using Micromeritics ASAP 2000 analyser. Elemental C and N were determined through the combustion carbon and nitrogen using LECO CN828 analyzer (Leco Corporation, St. Joseph, MI, USA).

The morphology of the copolymers was determined with a scanning electron microscopy (SEM) and transmission electron microscopy (TEM). The samples were covered with graphite and Pd/Au using an EMITECH K250X carbon evaporator. The captures were acquired using an FEI-QUANTA 200 Environment ESEM-EDS scanning electron microscope under voltage conditions of 20 kV at high vacuum, with Spot 4 and at a working distance of 10 mm using the secondary electron detector (ETD, Everhardt Thornley Detector) to see the surface image and the Solid-State backscatter electron detector (SSD, Solid- State Detector) to see the compositional difference in the removal of the metals. In addition, transmission electron microscopy was conducted utilizing the JEOL JEM 1400 equipment operating at a voltage of 100 kV.

2.5. Metal determination

Samples prepared with each heavy metal were measured in the atomic absorption spectrometer SpectrAA 50B (Varian). The standard calibration curves of $Cd(NO_3)_2{\cdot}4\ H_2O$, $Pb(NO_3)_2$, $Zn(NO_3)_2{\cdot}6\ H_2O$, Cu $(SO_4){\cdot}5\ H_2O$, and $Mn(SO_4){\cdot}H_2O$ were plotted by measuring the absorbance at 222.6, 228.8, 283.3, 213.9, and 403.1 nm, respectively. Absorbance values with a standard deviation>1% were discarded, and an average of the results was used. The linear working range was up to 100 ppm, except for zinc and cadmium, for which the linear working range was up to 20 ppm, and solutions were diluted as needed.

Samples prepared with mixes of heavy metals were filtered and diluted with 2% nitric acid trace metal grade. The equipment was calibrated by standard solutions (Agilent Technologies). Each element was determined by inductively coupled plasma mass spectrometry (ICP-MS, Agilent Technologies 7800) operated in He-HMI acquisition mode.

3. Results and discussion

3.1. Characterization of polysulfide

Several techniques were used to describe the structure of the copolymers: FTIR, ^{1}H NMR, solid ^{13}C NMR, zeta potential, nitrogen adsorption, elemental analysis, and SEM. Fig. 1A shows FTIR spectra of copolymers S/CO:80/20 and S/CO/TAA:80/14/6. As left in the study carried out by Cubero-Cardoso et al., [25], the signals of this type of copolymer with castor oil monomers and sulfur are described in detail. The hydroxyl group of CO appears at 2970 cm^{-1}, confirming the presence of ricinoleic acid. Other intense peaks appeared at 2930 and 2853 cm^{-1}, which arose from the asymmetric C-H stretching vibration in CH_3 and CH_2. The peak at 1740 cm^{-1} was attributed to a carbonyl group (C = O). For the copolymer S/CO/TAA:80/14/6, no new peak corresponding to the C = C bonds of triallylamine is observed.

Fig. 1S shows ^{1}H NMR spectra of the S/CO:80/20 and S/CO/

Table 1
A) Adsorption isotherm parameters and B) kinetic for the adsorption of Cd^{2+}, Pb^{2+}, Zn^{2+}, Mn^{2+} and Cu^{2+} varied time of removal.

A)						
Metal	Langmuir parameters			Freundlich parameters		
	q_{max} (mg/g)	k_L (L/mg)	R^2	n	k_F (mg/g)	R^2
Cd^{2+}	0.546	0.210	0.902	4.131	6.209	0.699
Pb^{2+}	0.851	0.191	0.939	4.065	11.907	0.802
Zn^{2+}	0.499	0.167	0.9263	5.112	5.767	0.595
Mn^{2+}	0.381	0.124	0.848	3.022	8.888	0.599
Cu^{2+}	0.649	0.259	0.901	4.653	6.014	0.759

B)						
Metal	Pseudo-first-order model			Pseudo-secondary-order model		
	$q_{e,\ calc}$ (mg/g)	k_1 (h^{-1})	R^2	$q_{e,\ calc}$ (mg/g)	k_2 (g/mg·h)	R^2
Cd^{2+}	1.163	0.024	0.873	2.107	0.12	0.987
Pb^{2+}	1.106	0.018	0.967	1.704	0.18	0.989
Zn^{2+}	–	–	–	0.859	−45.96	0.999
Mn^{2+}	–	–	–	0.243	−1.68	0.975
Cu^{2+}	1.432	0.018	0.521	1.967	13.44	0.987

TAA:80/14/6 copolymers. Similar to different studies, reaction monitoring was carried out in deuterated pyridine to obtain a good-quality solution, and reference peaks were observed at $\delta = 7.2$, $\delta = 7.6$, and $\delta = 8.7$ [37]. The S/CO:80/20 copolymer spectrum is similar to that described by [25]. In this work, solid-state ^{13}C NMR spectroscopy was performed on the S/CO:80/20 and S/CO/TAA:80/14/6 copolymers (Fig. 1B). Both copolymers exhibit a strong signal at $\delta = 68$, which arises from the C-O bond in glycerol [38]. Another signal at $\delta = 62$ can also be observed in both copolymers, which corresponds to the C-O bond in glycerol from castor oil triglyceride. However, this peak appears more intense in the S/CO/TAA:80/14/6 copolymer due to the overlap with a C-N peak. Fig. 1B shows double peaks at $\delta = 130$, representing C = C bonds, with more strength for S/CO/TAA:80/14/6. The double bonds from C = C show that the reaction is not complete from the non-opening double bond. The last, at $\delta = 172$, shows a peak corresponding to C = O.

The zeta potential of the two synthesized copolymers was determined and a slight difference was observed (**Fig. 2S**). The S/CO:80/20 copolymer had a value of -20.2 ± 1.9 mV, while the S/CO/TAA:80/14/6 copolymer was -26.2 ± 0.9 mV. This difference in zeta potential values may be attributed to the inclusion of heteroatoms in the end structure accompanied by a differing electrostatic distribution on the surface. Other studies have detected changes in the zeta potential, as shown in the case of carbon dots admitted into various heteroatoms [39]. The results of the gas adsorption analysis indicate that the polymers studied in this research do not exhibit significant microporosity, as has been observed in previous studies on copolymers with limonene synthesized by inverse vulcanization [32,40] (Fig. 1C, **Fig. 3S, and Table 2S**). Nonetheless, a slight variance is discernible between the polymers depending on the percentage of S_8. Specifically, the S/CO:80/20 and S/CO/TAA:80/14/6 copolymers exhibit a slightly larger difference than the S/CO:70/30 and S/CO:30/70 copolymers. According to the Brunauer-Emmett-Teller (BET) surface area analysis (**Table 1S**), there are no micropores that increase the surface area in the materials described, however it would be possible to effectively increase the specific surface using porogens in the synthesis of the copolymers [41]. The SEM and TEM images of different copolymers (Fig. 1D, F **4S**, and **5S**) exhibited a uniform dispersion of polyhedral nanoparticles, showcasing a crystalline appearance on the surface of the copolymers. In order to provide evidences about the atom distribution on the copolymer surface SEM-EDS analysis displays the elemental weight percentages of the copolymers, revealing differences between the copolymers synthesized with varying proportions of carbon and sulfur (Fig. 1E **and Table 3S**). In the case of the S/CO:80/20, S/CO:70/30 or S/CO:30/70 copolymers there are not nitrogen atom on their surface, however the spectrum of S/CO/TAA:80/14/6 copolymer exhibit nitrogen atoms on its composition (Fig. 1E). The copolymer was subjected to an elemental analysis to determine its nitrogen content (**Table 4S**). The expected nitrogen percentage, based on theoretical calculations, was 0.78% w/w. However, the actual measurement revealed a much lower nitrogen content of only 0.186% w/w. These results indicate that the copolymer's final structure contains a remarkably small amount of nitrogen.

3.2. Comparison of removal metal in water with different polysulfides.

A study was performed to compare different adsorbents synthesized, such as S/CO at 30/70, 70/30, and 80/20 (w/w %). Other adsorbents were compared with sulfur at 100% for 1 and 24 h with 1 g of adsorbent and 20 mL of different metal solutions at 100 mg/L (Fig. 2**A and B**). For times of one hour, the removal of the different metals was similar in the different S/CO copolymers; even with only 100% S_8 higher concentrations of metals were adsorbed than with the S/CO copolymers (Fig. 2A). The removal of metals with S/CO:80/20 copolymers was approximately 47%, 40%, 41% 19%, and 13% for Cd^{+2}, Pb^{2+}, Zn^{2+}, Mn^{2+}, and Cu^{2+}, respectively. These percentages have improved compared to those presented by Wu et al., [42], who removed less than 30% of the Pb^{2+} at 16 h. In Fig. 2B, significant effects have been shown when the adsorbent is in contact with the solution of different metals for 24 h. It has been observed that with the increase in the S/CO ratio the removal of metals increases, obtaining values of 78% for Cd, 82% for Pb, 38% for Zn^{2+}, and 73% for Cu^{2+} for the S/CO:80/20 copolymers. For Mn^{2+}, removal does not increase with an increased S/CO ratio, obtaining only 21% of removal. Similar studies using copolymers with sulfur have attempted to extract different metals in water solution, only obtaining significant removals with mercury [17,27,29,42–44].

The influence of dosages on S/CO:80/20 copolymer adsorption of heavy metals is shown in Fig. 2C. Different dosages were compared over 24 h with 1 g of S/CO:80/20 copolymers, and the volume of different metal solutions was changed to 100 mg/L for each metal. Fig. 2C shows how for all metals, except for Mn^{2+}, the increase in the dosages increases the elimination of the studied metals. With a 50% Polysulfide-Co-Cottonseed Oil, the same effect has been observed with increasing dosage on mercury removal [28]. In addition, a linear elimination relative to increasing dose was observed, reaching 100% for Cd^{2+} and 88% for Cu^{2+} and Pb^{2+} with a 100 mg/L dosage.

3.3. Kinetic study of the adsorption of different metals in water with the S/CO:80/20 copolymer

Different isotherm models, including the Langmuir isotherm and the Freundlich isotherm models, were used to investigate the relationship between heavy metal ions and the adsorbent. The best-fit isotherm model was selected based on the linear regression correlation coefficients, as seen in Table 1**A and B**. The Langmuir and Freundlich isotherm models were applied to the experimental equilibrium data for Cd^{2+}, Pb^{2+}, Zn^{2+}, Mn^{2+}, and Cu^{2+} adsorption by the S/CO:80/20 copolymer.

The values of the square of the correlation coefficient (R^2) were reported to indicate the goodness of the model fit. It was found that the data obtained from this study display deviations from linearity for the Freundlich isotherm. However, for the Langmuir isotherm, the correlation coefficients indicate that the data were well correlated, implying the applicability of this isotherm. On the one hand, the Freundlich isotherm model is suitable for multilayer adsorption on the surface of heterogeneous adsorbents, which assumes that the adsorption molecules are not uniformly distributed and have different affinities for the non-uniform adsorbent surface. On the other hand, the Langmuir isotherm model assumes that surface adsorption is a single layer, all adsorption sites are equal, and adsorbed ions are completely independent and do

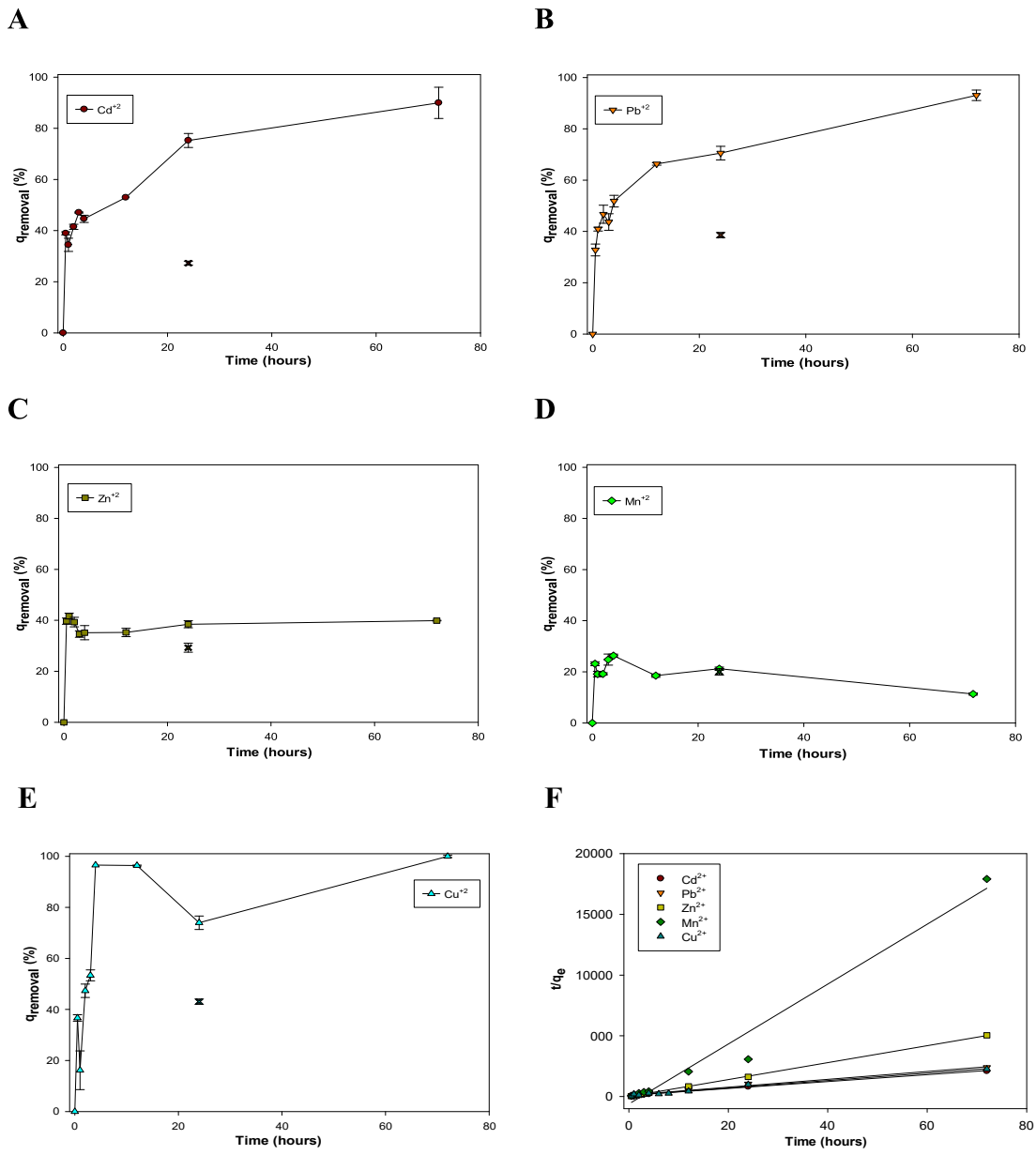

Fig. 3. Percentage of removal until 72 h by metal from water using S/CO:80/20 copolymer. All experiments were carried out using 1.0 g of the copolymer in 20 mL of the aqueous solution of metals A) Cd^{2+}, B) Pb^{2+}, C) Zn^{2+}, D) Mn^{2+} E) Cu^{2+} and F) representation of the equation of pseudo-secondary-order model. At 24 h of each graph (A-E) shows the adsorption of S_8.

not affect each other [45,46].

The maximum monolayer adsorption capacity removal using the S/CO:80/20 copolymer was found for Pb^{2+} and Cu^{2+}, i.e., 0.851 and 0.649 mg/g, respectively (Table 1A). It has been observed that for Cd^{2+} and Zn^{2+}, the adsorbent has less affinity, i.e., 0.546 and 0.499 mg/g, respectively (Table 1A). As seen in previous studies, Mn^{2+} has the lowest q_{max}, i.e., 0.381 mg/g, indicating that removal does not influence time (Table 1A).

The equilibrium parameter, R_L, of the Langmuir model was calculated using Ec. (9):

$$R_L = \frac{1}{1 + k_L \cdot C_0} \tag{9}$$

where Co (mg L^{-1}) is the initial concentration of the solution and k_L (L mg^{-1}) is the Langmuir isotherm coefficient. R_L describes the adsorption tendency, that is, adsorption is favorable when R_L is in the range of 0–1, irreversible when $R_L = 0$, linear when $R_L = 1$, and unfavorable when $R_L > 1$ [27]. The calculated values were between 0.04 and 0.89, corresponding to the first condition, which also indicates the suitability of the Langmuir model and affirms that the S/CO:80/20 copolymer was favorable for the adsorption of the different metals under the conditions of this study. Another parameter that evaluates whether the absorption of these metals is favorable is the sorption intensity parameter (n) of the Freundlich model. Values > 1 reflect a good process, and all the studies showed sorption intensity parameters of n > 3 [27].

Fig. 3 shows the removal efficiencies of the different metals measured from 0.5 to 72 h with 1 g of S/CO:80/20 copolymer and 20 mL of a 100 mg/L solution of each metal. As shown in Fig. 3E, the metal with the highest affinity for this copolymer is Cu^{2+}, removing of 97% at 4 h. Other metals with higher affinity are Cd^{2+} and Pb^{2+} with 90% and 93% at 72 h (Fig. 3**A and B**). Based on the Pearson theory, interactions between soft-acid and soft-base have been observed, affirming the affinity with heavy metals, such as Cu^{2+}, Cd^{2+} and Pb^{2+}, toward sulfur. [47]. However, this interaction is not as satisfactory for harder elements such

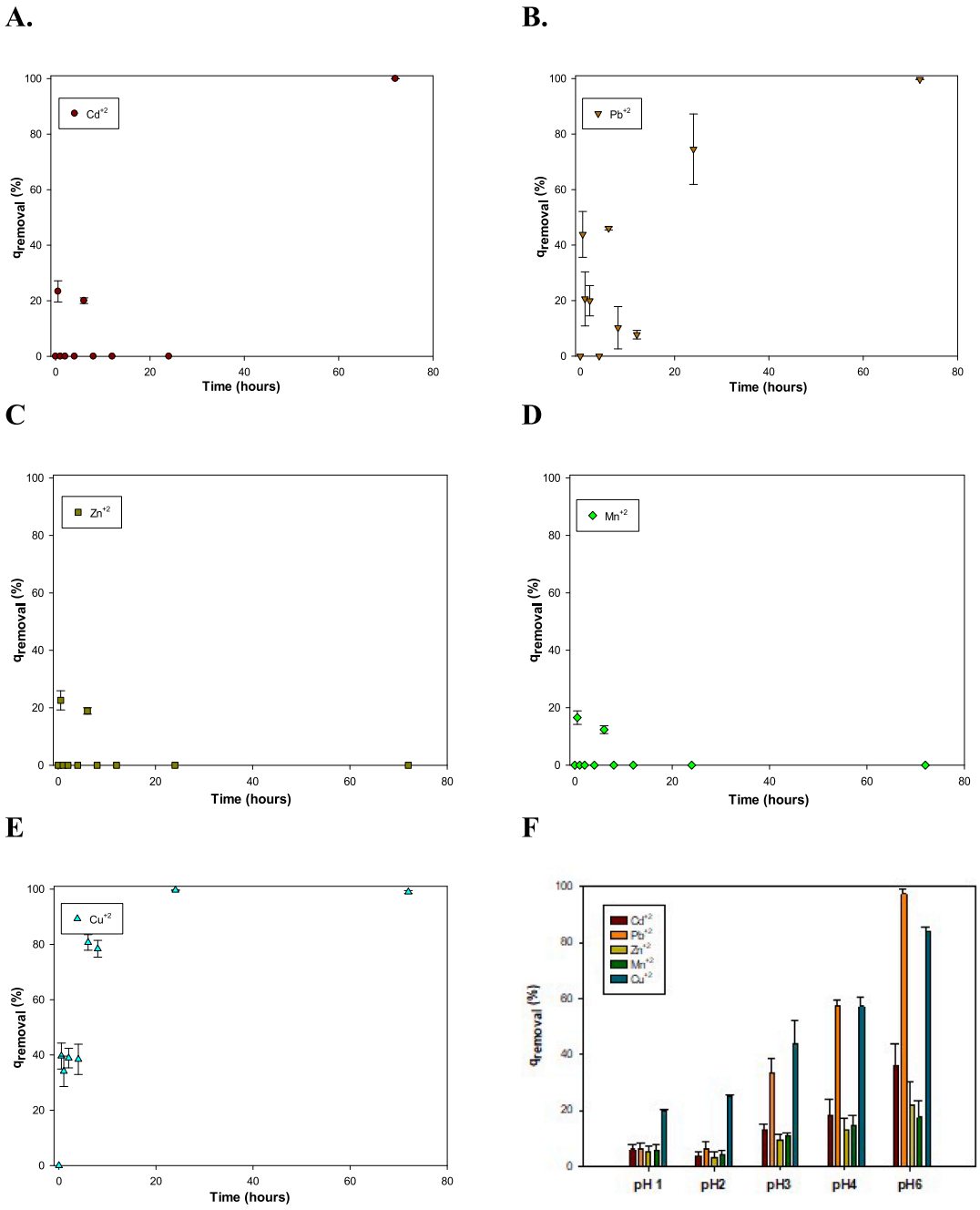

Fig. 4. Percentage of removal until 72 h by metal from water using S/CO:80/20 copolymer. All experiments were carried out using 1.0 g of the copolymer in 20 mL of the mix aqueous solution of metals A) Cd^{2+}= 6.9 ± 0.4 mg/L B) Pb^{2+}= 3.9 ± 0.1 mg/L, C) Zn^{2+}= 8.8 ± 0.6 mg/L, D) Mn^{2+}= 11.2 ± 0.3 mg/L, and E) Cu^{2+}= 6.5 ± 0.2 mg/L. F) Percentage of metals removal with S/CO:80/20 copolymer during 24 h at different pH.

as Zn^{2+} and Mn^{2+} and remains almost constant for all attempts. Fig. 3**C** and **D** show the adsorption of Zn^{2+} and Mn^{2+}, observing only adsorption of 40 and 25%, respectively. This study affirms the study carried out by Lundquist et al., [29], which demonstrated how Pb^{2+} was adsorbed with a sulfur copolymer and 50% canola oil. In addition, it has been observed how the copolymer based on inverse vulcanization attends to remove different heavy metals from water than mercury, which has been the most studied [27,43,48,49].

Table 1B shows the kinetic values of Eqs. (6) and (8) for the adsorption of each metal with the S/CO:80/20 copolymer. As shown in Table 1B, the pseudo-second order model fits the adsorption kinetics of each metal better because it has a higher R^2. According to Tikoalu et al., [27], adsorption with copolymers formed by inverse vulcanization has a chemisorption process since redox processes participate. The kinetic constant of the pseudo-second-order model shows that copper is the metal with the highest k_2, i.e., 13.44 g/mg·h (Table 1B**)**. Compared to cadmium and lead, they have much slower kinetics with k_2 values of 0.12 and 0.18 g/mg·h, respectively.

3.4. Study of the adsorption of mixed metals in water with the S/CO:80/20 copolymer

This study was carried out to preview the removal percentage of five metals in a mixed solution using S/CO copolymers. The mixed-metals solution presented values of pH = 2.7. Fig. 4**A–E** show the percentage of adsorption at 72 h of the metal ions Cd^{2+}, Pb^{2+}, and Cu^{2+} with

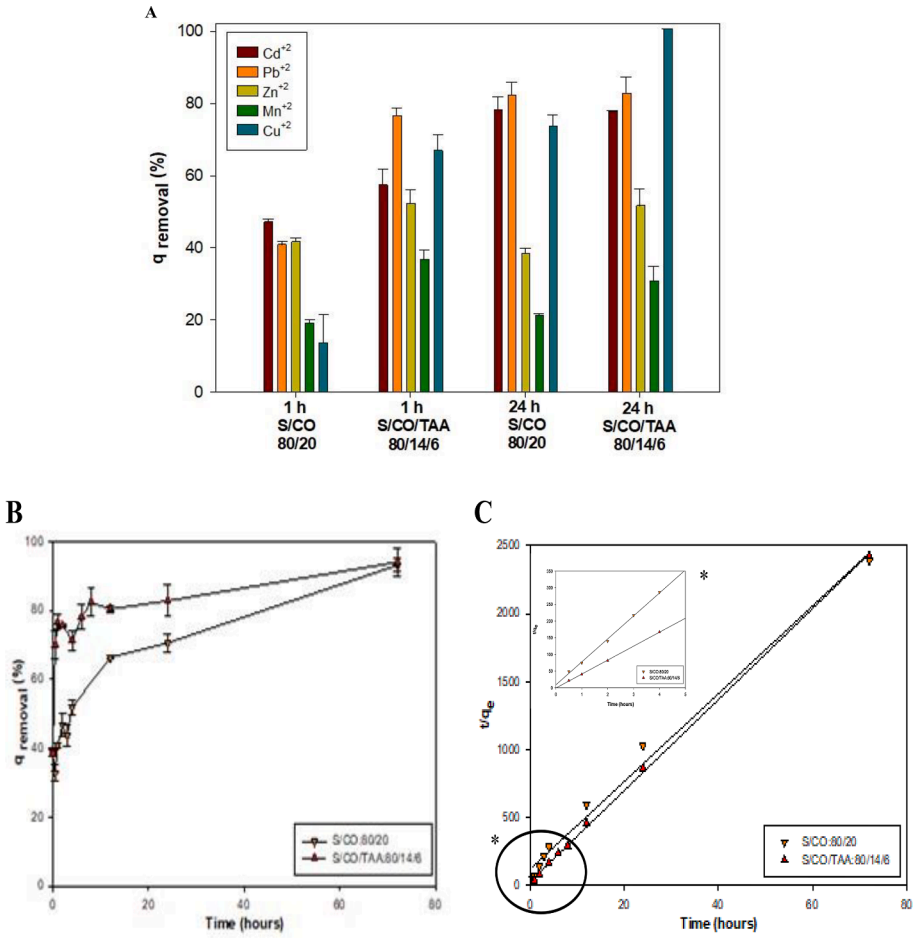

Fig. 5. A) Percentage of metals removal with different adsorbent from S/CO and S/CO/TAA copolymers during 1 h and 24 h. B) Percentage of removal lead until 72 using S/CO:80/20 and S/CO/TAA:80/14/6 copolymers. C) representation of the equation of pseudo-secondary-order model.

Table 2
Kinetic for the adsorption of Pb^{2+} using S/CO:80/20 and S/CO/TAA:80/14/6 copolymers.

Metal	Pseudo-first-order model			Pseudo-secondary-order model		
	$q_{e,\ calc}$	k_1	R^2	$q_{e,\ calc}$	k_2	R^2
	(mg/g)	(h^{-1})		(mg/g)	(g/mg·h)	
Pb	1.106	0.018	0.967	1.704	0.18	0.989
Pb/TAA	0.345	0.048	0.722	1.790	40.5	0.999

elimination percentages of 100.0 ± 0.0, 99.7 ± 0.0 and 99.0 ± 0.5%, respectively. Fig. 4**A–E** show how, at different times, an adsorption–desorption process occurs due to the competition between the metals and the specific surface of the copolymer. However, Mn^{2+} and Zn^{2+} adsorption only adsorbed approximately 20% in the early stages of the study. According to Pearson's theory, there are very effective interactions between soft acids and soft bases. Hence, sulfur is associated with heavy metals such as Pb^{2+} and Cd^{2+}. In the case of harder elements such as Mn^{2+} or Zn^{2+}, this interaction is not entirely satisfactory, and the average removal percentage remains stable. All tests were performed as

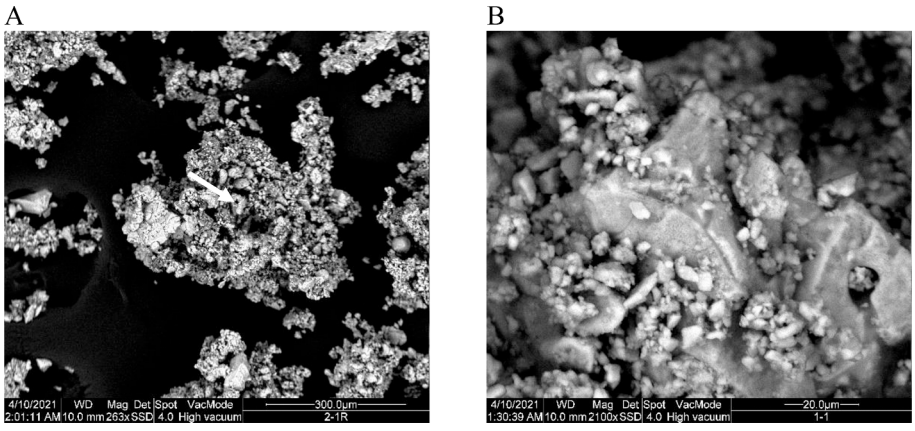

Fig. 6. Scanning electron microscope capture with SSD of the S/CO:80/20 copolymer (A) and the S/CO/TAA: 80/16/4 copolymer (B).

a function of time. The affinity of these heavy metals with the copolymer has also been observed in Cubero-Cardoso et al., [25]. According to a recent study, copolymers synthesized through inverse vulcanization, utilizing dioleyl[2,2′-bipyridine]-4,4′-dicarboxylate as comonomer and bicarbonate to increase porosity, have been found to possess high efficiencies in adsorbing a mixture of 11 metals [32].The study on the influence of pH can be seen where the removal of each metal at different pH values is represented (Fig. 4F). High pH values, up to pH 6, resulted in a higher percentage of metal removal. It will significantly improve the removal percentage of Pb^{2+} and Cu^{2+}. The literature shows that at pH levels >7, the removal of metal percentage becomes lower because they precipitate in the medium [33,50]. We can also observe a trend of Cd^{2+} improvements when the pH changes from 4 to 5, matching what was seen in the study by Qu et al., [33]. It is also observed that the optimal pH for the adsorption of metals with our copolymer would be pH 6, where the most significant amount of metal removal occurs. It can be verified that this is an optimal level to work with removing metals. We are demonstrating this optimality in studies such as the one by Akay et al., [50], where it can be seen that there is a higher level of adsorption when the pH increases to pH 6. In addition, it has been verified that for metals such as Pb^{2+}, the influence of pH is very significant for the increase in removal [47].

3.5. Effect of the new copolymer based on tryallylamine on metal adsorption from water

The copolymer synthesized with triallylamine was made to provide a new atom such as nitrogen. Obtaining a new copolymer with heteroatoms (S, C, O and N) makes the copolymer more adept at adsorbing heavy metals. N-containing functional groups can increase carbon surface polarity, and O-containing functional groups can increase acidity by facilitating interactions between carbon surfaces and target molecules [51]. Therefore, forming new copolymers with heteroatoms of functional groups, such as nitrogen, oxygen, and sulfur, can be more effective in adsorption activity. A study was performed to compare different adsorbents synthesized S/CO:80/20 (w/w %) and S/CO/TAA:80/14/6 (w/w/w %). These adsorbents were reached during 1 and 24 h with 1 g of adsorbent and 20 mL of different metal solutions at 100 mg/L (Fig. 5A). A great variation is shown with the S/CO/TAA copolymers concerning S/CO:80/20 copolymers over 1 h, increasing by 10%, 24%, 13%, 17% 17%, and 53% for Cd^{2+}, Pb^{2+}, Zn^{2+}, Mn^{2+}, and Cu^{2+}, respectively. In addition, removal increased at 24 h with the S/CO/TAA copolymers compared to the S/CO:80/20 copolymers, increasing by 17%, 13%, 10%, and 26% for Pb^{2+}, Zn^{2+}, Mn^{2+}, and Cu^{2+}, respectively, although Cd^{2+} did not increase with respect to the S/CO copolymers.

The kinetic study was carried out from Pb^{2+} with the S/CO/TAA:80/14/6 copolymer, observing an increase concerning the S/CO:80/20 copolymer (Fig. 5**B and C**). As shown in Fig. 5B, the adsorption of Pb^{2+} has faster kinetics with the copolymer S/CO/TAA:80/14/6 copolymer. The S/CO:80/20 copolymer removed 40% at one hour, while the S/CO/TAA:80/14/6 copolymer achieved 76% removal at one hour. However, for both copolymers, the maximum adsorption was at 72 h with an elimination of 93% for both. In addition, the kinetic constant of the pseudo-second order model shows that the S/CO/TAA:80/14/6 copolymer has a higher rate constant than the S/CO:80/20 copolymer, i.e., 40.5 g/mg·h in S/CO/TAA:80/14/6 with respect to the S/CO:80/20 copolymer with 0.18 g/mg·h (Fig. 5**B** and Table 2**)**.

Samples of the S/CO:80/20 copolymer and the S/COO/TAA: 80/14/6 copolymer after the lead adsorption process were observed under the SEM microscope with SSD (Fig. 6). In the images taken with ETD, it is observed that the S/CO:80/20 copolymer is more porous than the S/COO/TAA: 80/14/6 copolymer (**Fig. 6S**). In addition, small crystalline and smoother particles are observed on the surfaces of the two copolymers identified as free sulfur in other studies [19,27,43]. The S/COO/TAA: 80/14/6 copolymer was the copolymer that eliminated more lead, as we have seen previously. This fact is also observed when we see more particles with a clearer intensity on the surfaces of this copolymer concerning the S/CO:80/20 copolymer (Fig. 6**A and B**).

4. Conclusions

In this study, sustainable hybrid copolymers were synthesized using castor oil, triallylamine, and sulfur through the inverse vulcanization method. The copolymers were fully characterized using FTIR, ^{1}H NMR, solid ^{13}C NMR, zeta potential, nitrogen adsorption, Elemental analysis, TEM, and SEM to determine their structure and the presence of heteroatoms such as nitrogen in the final structure. The study demonstrated a simple strategy to adjust the copolymer structure for maximum affinity towards various metals in the solution. The optimal conditions for removing metals in water were observed with S/CO:80/20 and S/CO/TAA:80/14/6 copolymers, which showed better affinity towards soft heavy metals. The addition of a third comonomer with nitrogen significantly improved removal performance and kinetic parameters, highlighting the potential of ternary hybrid copolymers for water remediation.

Funding

The authors are grateful to the Regional Government of Andalusia, Junta de Andalucía, Consejería de Economía y Conocimiento (Project UHU-1257728).

Declaration of competing interest

The authors declare no conflict of interest, and the funders had no role in the design of the study; in the collection, analyses, or interpretation of data; in the writing of the manuscript; or in the decision to publish the results.

CRediT authorship contribution statement

Amanda Haro-Martínez: Methodology, Writing – original draft. **Rocío Arroyo-Carrasco:** Methodology. **Laura Galván:** Conceptualization, Resources, Writing – review & editing. **Ana Sayago:** Resources, Writing – review & editing. **Antonio A. Cuadri:** Funding acquisition. **José Enrique Martín-Alfonso:** Funding acquisition. **Ángeles Trujillo-Reyes:** Methodology, Writing – review & editing. **Fernando G. Fermoso:** Writing – review & editing. **Juan Cubero-Cardoso:** Conceptualization, Methodology, Writing – original draft. **Juan Urbano:** Conceptualization, Methodology, Resources, Writing – review & editing, Supervision, Funding acquisition.

Declaration of Competing Interest

The authors declare that they have no known competing financial interests or personal relationships that could have appeared to influence the work reported in this paper.

Data availability

No data was used for the research described in the article.

Acknowledgments

The authors also want to express their acknowledgement of Fundación Cátedra Cepsa for kindly supplying the sulfur and the group FQM-383 “Nanoquímica y valorización de residuos y biomasa” (NANOVAL), CITIUS from US and SCAI from UCO for facilities. We also wish to thank the referees for their valuable contributions. Funding for open access charge: University of Huelva / CBUA.

Appendix A. Supplementary data

Supplementary data to this article can be found online at https://doi.org/10.1016/j.cej.2023.143905.

References

[1] M. Khodakarami, M. Bagheri, Recent advances in synthesis and application of polymer nanocomposites for water and wastewater treatment, J. Clean. Prod. 296 (2021), 126404, https://doi.org/10.1016/j.jclepro.2021.126404.

[2] D. Ma, H. Yi, C. Lai, X. Liu, X. Huo, Z. An, L. Li, Y. Fu, B. Li, M. Zhang, L. Qin, S. Liu, L. Yang, Critical review of advanced oxidation processes in organic wastewater treatment, Chemosphere. 275 (2021), 130104, https://doi.org/10.1016/j.chemosphere.2021.130104.

[3] Directive 2000/60/EC, DIRECTIVE 2000/60/EC Establishing a framework for Community action in the field of water policy, 2000.

[4] K. He, S. Wang, Y. Liu, Z. Cao, L. Yang, F. He, Enhanced removal of hexavalent chromium by lignosulfonate modified zero valent iron: Reaction kinetic, performance and mechanism, Sci. Total Environ. 857 (2023), 159397, https://doi.org/10.1016/J.SCITOTENV.2022.159397.

[5] L. Wang, Z. Li, Y. Wang, P.C. Brookes, F. Wang, Q. Zhang, J. Xu, X. Liu, Performance and mechanisms for remediation of Cd(II) and As(III) co-contamination by magnetic biochar-microbe biochemical composite: Competition and synergy effects, Sci. Total Environ. 750 (2021), 141672, https://doi.org/10.1016/J.SCITOTENV.2020.141672.

[6] T.C. Egbosiuba, A.S. Abdulkareem, A.S. Kovo, E.A. Afolabi, J.O. Tijani, M. T. Bankole, S. Bo, W.D. Roos, Adsorption of Cr(VI), Ni(II), Fe(II) and Cd(II) ions by KIAgNPs decorated MWCNTs in a batch and fixed bed process, Sci. Rep. 11 (2021) 75, https://doi.org/10.1038/s41598-020-79857-z.

[7] M.T. Amin, A.A. Alazba, U. Manzoor, A review of removal of pollutants from water/wastewater using different types of nanomaterials, Adv. Mater. Sci. Eng. 2014 (2014) 1–24.

[8] R. Benson, O.D. Conerly, W. Sander, A.L. Batt, J.S. Boone, E.T. Furlong, S. T. Glassmeyer, D.W. Kolpin, H.E. Mash, K.M. Schenck, J.E. Simmons, Human health screening and public health significance of contaminants of emerging concern detected in public water supplies, Sci. Total Environ. 579 (2017) 1643–1648.

[9] A. Sharma, P. Kumar Sharma, R. Malviya, Role of different parameters and mathematical models for metal ions adsorption from industrial waste water, Biointerface Res. Appl. Chem. 10 (2020) 5556–5563.

[10] M.L. Soto, A. Moure, H. Domínguez, J.C. Parajó, Recovery, concentration and purification of phenolic compounds by adsorption: A review, J. Food Eng. 105 (2011) 1–27, https://doi.org/10.1016/j.jfoodeng.2011.02.010.

[11] N. Qiu, S. Guo, Y. Chang, Study upon kinetic process of apple juice adsorption decoloration by using adsorbent resin, J. Food Eng. 81 (2007) 243–249, https://doi.org/10.1016/j.jfoodeng.2006.10.030.

[12] C. Tejada-Tovar, Á. Villabona-Ortiz, L. Garcés-Jaraba, Adsorción de metales pesados en aguas residuales usando materiales de origen biológico, TecnoLógicas. 18 (2015) 109. https://doi.org/10.22430/22565337.209.

[13] V.K. Gupta, I. Ali, T.A. Saleh, A. Nayak, S. Agarwal, Chemical treatment technologies for waste-water recycling - An overview, RSC Adv. 2 (16) (2012) 6380.

[14] W.J. Chung, A.G. Simmonds, J.J. Griebel, E.T. Kim, H.S. Suh, I.B. Shim, R.S. Glass, D.A. Loy, P. Theato, Y.E. Sung, K. Char, J. Pyun, Elemental sulfur as a reactive medium for gold nanoparticles and nanocomposite materials, Angew. Chemie - Int. Ed. 50 (2011) 11409–11412, https://doi.org/10.1002/anie.201104237.

[15] J.J. Griebel, R.S. Glass, K. Char, J. Pyun, Polymerizations with elemental sulfur: A novel route to high sulfur content polymers for sustainability, energy and defense, Prog. Polym. Sci. 58 (2016) 90–125, https://doi.org/10.1016/j.progpolymsci.2016.04.003.

[16] P.T. Anastas, M.M. Kirchhoff, Origins, current status, and future challenges of green chemistry, Acc. Chem. Res. 35 (2002) 686–694, https://doi.org/10.1021/ar010065m.

[17] M.J.H. Worthington, R.L. Kucera, J.M. Chalker, Green chemistry and polymers made from sulfur, Green Chem. 19 (2017) 2748–2761, https://doi.org/10.1039/c7gc00014f.

[18] H. Berk, M. Kaya, M. Topcuoglu, N. Turkten, Y. Karatas, A. Cihaner, Synthesis, characterization and application of high sulfur content polymeric materials from fatty acids, React. Funct. Polym. 187 (2023), 105581, https://doi.org/10.1016/J.REACTFUNCTPOLYM.2023.105581.

[19] A. Hoefling, Y.J. Lee, P. Theato, Sulfur-Based Polymer Composites from Vegetable Oils and Elemental Sulfur: A Sustainable Active Material for Li–S Batteries, Macromol. Chem. Phys. 218 (1) (2017) 1600303.

[20] S.F. Valle, A.S. Giroto, R. Klaic, G.G.F. Guimarães, C. Ribeiro, Sulfur fertilizer based on inverse vulcanization process with soybean oil, Polym. Degrad. Stab. 162 (2019) 102–105, https://doi.org/10.1016/j.polymdegradstab.2019.02.011.

[21] J.A. Smith, R. Mulhall, S. Goodman, G. Fleming, H. Allison, R. Raval, T. Hasell, Investigating the Antibacterial Properties of Inverse Vulcanized Sulfur Polymers, ACS Omega. 5 (2020) 5229–5234, https://doi.org/10.1021/acsomega.9b04267.

[22] J. Cubero-Cardoso, P. Gómez-Villegas, M. Santos-Martín, A. Sayago, Á. Fernández-Recamales, R. Fernández de Villarán, A.A. Cuadri, J.E. Martín-Alfonso, R. Borja, F. G. Fermoso, R. León, J. Urbano, Combining vegetable oils and bioactive compounds via inverse vulcanization for antioxidant and antimicrobial materials, Polym. Test. 109 (2022), 107546, https://doi.org/10.1016/j.polymertesting.2022.107546.

[23] K. Wei, K. Zhao, Y. Gao, H. Zhang, X. Yu, M.-H. Li, J. Hu, Near-infrared-light responsive degradable polysulfide pesticide carriers by one-pot inverse vulcanization, Chem. Eng. J. 462 (2023), 142191, https://doi.org/10.1016/J.CEJ.2023.142191.

[24] H. Shen, H. Qiao, H. Zhang, Sulfur-urushiol copolymer: A material synthesized through inverse vulcanization from renewable resources and its latent application as self-repairable and antimicrobial adhesive, Chem. Eng. J. 450 (2022), 137905, https://doi.org/10.1016/J.CEJ.2022.137905.

[25] J. Cubero-Cardoso, A.A. Cuadri, F.G. Fermoso, J.E. Martín-Alfonso, J. Urbano, Promising Chalcogenide Hybrid Copolymers for Sustainable Applications as Bio-lubricants and Metal Adsorbents, ACS Appl. Polym. Mater. 4 (2022) 3667–3675, https://doi.org/10.1021/acsapm.2c00209.

[26] F.G. Müller, L.S. Lisboa, J.M. Chalker, Inverse Vulcanized Polymers for Sustainable Metal Remediation, Adv. Sustain. Syst. 7 (2023) 2300010, https://doi.org/10.1002/ADSU.202300010.

[27] A.D. Tikoalu, N.A. Lundquist, J.M. Chalker, Mercury Sorbents Made By Inverse Vulcanization of Sustainable Triglycerides: The Plant Oil Structure Influences the Rate of Mercury Removal from Water, Adv. Sustain. Syst. 4 (2020) 1–9, https://doi.org/10.1002/adsu.201900111.

[28] Y. Chen, A. Yasin, Y. Zhang, X. Zan, Y. Liu, L. Zhang, Preparation and modification of biomass-based functional rubbers for removing mercury(II) from aqueous solution, Materials (Basel). 13 (3) (2020) 632.

[29] N.A. Lundquist, J.M. Chalker, Confining a spent lead sorbent in a polymer made by inverse vulcanization prevents leaching, Sustain. Mater. Technol. 26 (2020) e00222.

[30] A. Leon-Vaz, J. Cubero-Cardoso, Á. Trujillo-Reyes, F.G. Fermoso, R. León, C. Funk, J. Vigara, J. Urbano, Enhanced wastewater bioremediation by a sulfur-based copolymer as scaffold for microalgae immobilization (AlgaPol), Chemosphere. 315 (2023), 137761, https://doi.org/10.1016/J.CHEMOSPHERE.2023.137761.

[31] L.A. Limjuco, G.M. Nisola, K.J. Parohinog, K.N.G. Valdehuesa, S.P. Lee, H. Kim, W. J. Chung, Water-insoluble hydrophilic polysulfides as microfibrous composites towards highly effective and practical Hg2+ capture, Chem. Eng. J. 378 (2019), 122216, https://doi.org/10.1016/j.cej.2019.122216.

[32] L.A. Ko, Y.S. Huang, Y.A. Lin, Bipyridine-Containing Polysulfide Materials for Broad-Spectrum Removal of Heavy Metals from Water, ACS Appl. Polym. Mater. 3 (2021) 3363–3372, https://doi.org/10.1021/ACSAPM.1C00259/SUPPL_FILE/AP1C00259_SI_001.PDF.

[33] J. Qu, X. Meng, X. Jiang, H. You, P. Wang, X. Ye, Enhanced removal of Cd(II) from water using sulfur-functionalized rice husk: Characterization, adsorptive performance and mechanism exploration, J. Clean. Prod. 183 (2018) 880–886, https://doi.org/10.1016/j.jclepro.2018.02.208.

[34] M. Iqbal, R.A. Khera, Adsorption of copper and lead in single and binary metal system onto Fumaria indica biomass, accessed March 14, 2022, Chem. Int. 1 (2015) 157b–163b, http://bosaljournals.com/chemint/.

[35] S.K. Lagergren, About the Theory of So-called Adsorption of Soluble Substances, accessed April 20, 2021, Sven. Vetenskapsakad. Handingarl. 24 (1898) 1–39, https://cir.nii.ac.jp/crid/1570009750361875328.bib?lang=en.

[36] Y.S. Ho, G. McKay, Comparative sorption kinetic studies of dye and aromatic compounds onto fly ash, J. Environ. Sci. Heal. Part A. 34 (1999) 1179–1204, https://doi.org/10.1080/10934529909376889.

[37] S.J. Tonkin, C.T. Gibson, J.A. Campbell, D.A. Lewis, A. Karton, T. Hasell, J. M. Chalker, Chemically induced repair, adhesion, and recycling of polymers made by inverse vulcanization, Chem. Sci. 11 (2020) 5537–5546, https://doi.org/10.1039/d0sc00855a.

[38] F. Lia B. Vella M. Zammit Mangion C. Farrugia Application of 1H and 13C NMR Fingerprinting as a Tool for the Authentication of Maltese Extra Virgin Olive Oil Foods 9 6 689.

[39] P. Ezati, J.W. Rhim, R. Molaei, R. Priyadarshi, S. Roy, S. Min, Y.H. Kim, S.G. Lee, S. Han, Preparation and characterization of B, S, and N-doped glucose carbon dots: Antibacterial, antifungal, and antioxidant activity, Sustain. Mater. Technol. 32 (2022) e00397.

[40] J.C. Bear, J.D. McGettrick, I.P. Parkin, C.W. Dunnill, T. Hasell, Porous carbons from inverse vulcanised polymers, Microporous Mesoporous Mater. 232 (2016) 189–195, https://doi.org/10.1016/J.MICROMESO.2016.06.021.

[41] S. Petcher, D.J. Parker, T. Hasell, Macroporous sulfur polymers from a sodium chloride porogen - A low cost, versatile remediation material, Environ. Sci. Water Res. Technol. 5 (2019) 2142–2149, https://doi.org/10.1039/c9ew00477g.

[42] X. Wu, J.A. Smith, S. Petcher, B. Zhang, D.J. Parker, J.M. Griffin, T. Hasell, Catalytic inverse vulcanization, Nat. Commun. 10 (2019) 1–9, https://doi.org/10.1038/s41467-019-08430-8.

[43] M.J.H. Worthington, R.L. Kucera, I.S. Albuquerque, C.T. Gibson, A. Sibley, A. D. Slattery, J.A. Campbell, S.F.K. Alboaiji, K.A. Muller, J. Young, N. Adamson, J. R. Gascooke, D. Jampaiah, Y.M. Sabri, S.K. Bhargava, S.J. Ippolito, D.A. Lewis, J. S. Quinton, A.V. Ellis, A. Johs, G.J.L. Bernardes, J.M. Chalker, Laying Waste to Mercury: Inexpensive Sorbents Made from Sulfur and Recycled Cooking Oils, Chem. - A Eur. J. 23 (2017) 16219–16230, https://doi.org/10.1002/chem.201702871.

[44] M.J.H. Worthington, C.J. Shearer, L.J. Esdaile, J.A. Campbell, C.T. Gibson, S. K. Legg, Y. Yin, N.A. Lundquist, J.R. Gascooke, I.S. Albuquerque, J.G. Shapter, G. G. Andersson, D.A. Lewis, G.J.L. Bernardes, J.M. Chalker, Sustainable Polysulfides for Oil Spill Remediation: Repurposing Industrial Waste for Environmental Benefit, Adv. Sustain. Syst. 2 (2018) 1800024, https://doi.org/10.1002/adsu.201800024.

[45] H. Jiang, Y. Yang, Z. Lin, B. Zhao, J. Wang, J. Xie, A. Zhang, Preparation of a novel bio-adsorbent of sodium alginate grafted polyacrylamide/graphene oxide hydrogel

for the adsorption of heavy metal ion, Sci. Total Environ. 744 (2020), 140653, https://doi.org/10.1016/j.scitotenv.2020.140653.
[46] T.H. Tran, A.H. Le, T.H. Pham, D.T. Nguyen, S.W. Chang, W.J. Chung, D. D. Nguyen, Adsorption isotherms and kinetic modeling of methylene blue dye onto a carbonaceous hydrochar adsorbent derived from coffee husk waste, Sci. Total Environ. 725 (2020), 138325, https://doi.org/10.1016/j.scitotenv.2020.138325.
[47] D. Saha, S. Barakat, S.E. Van Bramer, K.A. Nelson, D.K. Hensley, J. Chen, Noncompetitive and Competitive Adsorption of Heavy Metals in Sulfur-Functionalized Ordered Mesoporous Carbon, ACS Appl. Mater. Interfaces. 8 (2016) 34132–34142, https://doi.org/10.1021/acsami.6b12190.
[48] M.W. Thielke, L.A. Bultema, D.D. Brauer, B. Richter, M. Fischer, P. Theato, Rapid Mercury(II) removal by electrospun sulfur copolymers, Polymers (Basel). 8 (2016) 1–9, https://doi.org/10.3390/polym8070266.
[49] V.S. Wadi, H. Mittal, E. Fosso-Kankeu, K.K. Jena, S.M. Alhassan, Mercury removal by porous sulfur copolymers: Adsorption isotherm and kinetics studies, Colloids Surfaces A Physicochem. Eng. Asp. 606 (2020), 125333, https://doi.org/10.1016/j.colsurfa.2020.125333.
[50] S. Akay, B. Kayan, D. Kalderis, M. Arslan, Y. Yagci, B. Kiskan, Poly(benzoxazine-co-sulfur): An efficient sorbent for mercury removal from aqueous solution, J. Appl. Polym. Sci. 134 (2017) 1–11, https://doi.org/10.1002/app.45306.
[51] Y. Du, H. Chen, X. Xu, C. Wang, F. Zhou, Z. Zeng, W. Zhang, L. Li, Surface modification of biomass derived toluene adsorbent: hierarchically porous characterization and heteroatom doped effect, Microporous Mesoporous Mater. 293 (2020), 109831, https://doi.org/10.1016/J.MICROMESO.2019.109831.